

Heteronuclear Decoupling by Multiple Rotating Frame Technique

Haribabu Arthanari ^{*}, G. Wagner ^{*}, Navin Khaneja [†]

June 18, 2010

Abstract

The paper describes the multiple rotating frame technique for designing modulated rf-fields, that perform broadband heteronuclear decoupling in solution NMR spectroscopy. The decoupling is understood by performing a sequence of coordinate transformations, each of which demodulates a component of the Rf-field to a static component, that progressively averages the chemical shift and dipolar interaction. We show that by increasing the number of modulations in the decoupling field, the ratio of dispersion in the chemical shift to the strength of the rf-field is successively reduced in progressive frames. The known decoupling methods like continuous wave decoupling, TPPM etc, are special cases of this method and their performance improves by adding additional modulations in the decoupling field. The technique is also expected to find use in designing decoupling pulse sequences in Solid State NMR spectroscopy and design of various excitation, inversion and mixing sequences.

^{*}Harvard Medical School

[†]To whom correspondence may be addressed. Email:navin@hrl.harvard.edu. School of Engineering and Applied Sciences, Harvard University, Cambridge, MA 02138.

1 Introduction

Heteronuclear decoupling methods have a long history in NMR spectroscopy [1, 2, 3, 4, 5, 6, 7, 8, 9, 10, 11, 12, 13, 14, 15, 16, 17, 18, 19, 20, 21, 22, 23, 24, 25, 26, 27, 28, 29, 30] and *in vivo* applications [31, 32, 33, 34, 35, 36]. The goal of broadband heteronuclear decoupling sequences is to observe a spin S by irradiating spin I that is coupled to S in order to simplify the spectra and to increase the signal-to-noise ratio. At the same time, the decoupling sequence should introduce only a minimal amount of artifacts, such as decoupling sidebands. Furthermore, in order to avoid undesirable sample heating or damage to the probe, the radio frequency (rf) power of the decoupling sequence should be as small as possible. This is of particular importance in medical imaging or *in vivo* spectroscopy of humans [31, 32, 33, 34, 35, 36].

The earliest heteronuclear decoupling methods were based on cw irradiation [10] and noise decoupling [12]. Significantly improved decoupling sequences were found based on composite [8, 9, 13, 14, 16, 17, 18, 19] or shaped [24, 25, 26, 27, 28, 30] inversion pulses in combination with highly compensated cycles and supercycles [8, 9, 16, 37, 38, 39, 40, 41, 42, 43]. Theoretical approaches that have been used for the analysis and design of decoupling sequences include average Hamiltonian [15, 44, 45] and Floquet [29, 30] theory.

Here, we introduce a powerful approach for the design of heteronuclear decoupling sequences based on multiple rotating frame technique.

In the absence of chemical shifts, the most straightforward way to decouple two heteronuclear spins I and S is to just irradiate with full power on resonance to spin I . The presence of large chemical shifts makes this not the best strategy as using a CW irradiation, one creates an effective field that is not perpendicular to the coupling interaction and therefore part of the coupling interaction, parallel to this field is not averaged. We show that it is possible to design a multiply modulated rf-field, whose effect is best understood by performing a sequence of coordinate transformations, *specific to each chemical shift*. Each transformation reduces the chemical shift interaction and averages part of the coupling until the chemical shifts are made arbitrarily small. Each transformation demodulates a component of the multiply-

modulated rf-field to a static component. The subsequent transformation is in the rotating frame defined by new static component and the residual chemical shift. We show that by increasing the number of modulations in the decoupling field, we can significantly improve the decoupling. Methods to make this method robust to rf-inhomogeneity are discussed.

2 Heteronuclear Decoupling

Consider two heteronuclear spins I and S . The Hamiltonian of the spin system takes the form

$$H_0 = \omega_I I_z + 2\pi J I_z S_z + \omega_S S_z, \quad (1)$$

where ω_I and ω_S are the chemical shifts of spin I and S . Assuming spin S is being observed, we can without loss of generality take the chemical shift of the spin S to be zero and denoting $\omega_I = \omega_0$, consider the natural Hamiltonian

$$H_0 = \underbrace{\omega_0 I_z}_{H_{cs}} + \underbrace{2\pi J I_z S_z}_{H_c}, \quad (2)$$

where $\omega_0 \in [-c_0, c_0]$. Now, consider the rf-Hamiltonian

$$H'_0 = w_0 I_x + (w_1 \sin v_1 t + w_2 \cos v_1 t \sin v_2 t + \dots) I_y. \quad (3)$$

A more general form of the rf-Hamiltonian is then

$$H'_0 = w_0 I_x + \underbrace{\left(\sum_{k=1}^N w_k \prod_{j=1}^{k-1} \cos v_j t \sin v_k t \right)}_{A_0(t)} I_y. \quad (4)$$

where $v_k > v_{k+1}$. We adopt the notation $\bar{w}_k = 2^{-k} w_k$, and rewrite

$$H_0 = \tilde{\omega} I_{z_1(\omega)} + A_0(t) I_y + 2\pi J I_z S_z, \quad (5)$$

where $z_1(\omega)$ is the unit vector along the direction $\omega\hat{z} + w_0\hat{x}$ and define $\theta_1(\omega) = \tan^{-1}(\frac{w_0}{\omega})$, the spread of frequencies $\tilde{\omega} \in [w_0, \sqrt{w_0^2 + c_0^2}]$. Note, $z_1(\omega)$, is different for each ω . Now, by choosing v_1 in the first transformation as exactly the center of this spread and transforming into a frame rotating around $I_{z_1(\omega)}$, with frequency v_1 , we get the Hamiltonian

$$H_1 = \underbrace{(\tilde{\omega} - v_1)}_{f_1(\omega)} I_{z_1(\omega)} + 2\pi J \cos \theta_1(\omega) I_{z_1(\omega)} S_z + \underbrace{\bar{w}_1 I_{x_1} + A_1(t) I_y}_{H'_1} + H''_1(t) + H'''_1, \quad (6)$$

where H'_1 is the demodulated part of the Rf-Hamiltonian H'_0 , in the interaction frame of $I_{z_1(\omega)}$, that resembles H'_0 by design. $H''_1(t)$ and $H'''_1(t)$ are the fast oscillating parts of the rf and coupling Hamiltonian that we ideally want to average out and we neglect these terms for now. $H'''_1(t)$ is simply the part of the coupling perpendicular to the effective field direction $I_{z_1(\omega)}$, that oscillates with frequency v_1 . The new frequency $f_1(\omega) \in [-c_1, c_1]$, where $c_1 < c_0$. A_1 , H''_1 and H'''_1 are written in their general form below. The system obtained after first coordinate transformation has the desired feature that the ratio of chemical shift spread to Rf-strength $\alpha_1 = \frac{c_1}{\bar{w}_1}$ is reduced over $\alpha_0 = \frac{c_0}{w_0}$ for the original system. For example, if $c_0 = w_0$, then $\frac{c_1}{\bar{w}_1} = \sqrt{2} - 1$.

We can now iterate the above construction. We go into successive rotating frames around axis $I_{z_k(\omega)}$ with frequency v_k . Unit vectors $(x_k(\omega), y_k(\omega), z_k(\omega))$ define the k^{th} frame, where we suppress the argument ω subsequently. $f_k(\omega)$ is the chemical shift in the k^{th} rotating frame, starting with ω in H_0 . c_k represents the limit of the chemical shifts in the k^{th} coordinate frame and $\bar{w}_k = 2^{-k} w_k$ is the strength of the rf-field along the direction x_k .

$$H_k = f_k(\omega) I_{z_k(\omega)} + \frac{w_k}{2^k} I_{x_k} + 2\pi J_k I_{z_k} S_z + A_k(t) I_y + H''_k(t) + H'''_k(t), \quad (7)$$

$$A_k(t) = \frac{1}{2^k} \left\{ \sum_{m=k+1}^n w_m \prod_{i=k+1}^{m-1} \cos(v_i t) \sin(v_m t) \right\} I_y, \quad (8)$$

$$H''_k(t) = \exp(i2v_k I_{z_k} t) \left(-\frac{w_k}{2^k} I_{x_k} + A_k(t) I_y \right) \exp(-i2v_k I_{z_k} t), \quad (9)$$

$$H_k'''(t) = J_k \exp(iv_k I_{z_k} t) I_{x_k} S_z \exp(-iv_k I_{z_k} t) \quad (10)$$

$$c_{k+1} = \frac{\sqrt{c_k^2 + \bar{w}_k^2} - \bar{w}_k}{2}; \quad v_{k+1} = \frac{\sqrt{c_k^2 + \bar{w}_k^2} + \bar{w}_k}{2}; \quad \tan \theta_k(\omega) = \frac{\bar{w}_k}{f_k(\omega)} \quad (11)$$

$$J_k = \prod_{k=1}^n \cos \theta_k(\omega) J. \quad (12)$$

As discussed in the next section the iterated relations on c_k insures that the ratio $\alpha_k = \frac{c_k}{\bar{w}_k}$ is decreasing and $\theta_k \rightarrow \frac{\pi}{2}$. This ensures that $J_k \rightarrow 0$.

3 Scaling

To fix ideas, we choose $w_k = w_0$, i.e., $\bar{w}_k = 2^{-k} w_0$. From equation (11), we have the relation,

$$\alpha_{k+1} = \sqrt{1 + \alpha_k^2} - 1 < \alpha_k. \quad (13)$$

This ensures that α_k is decreasing. We explore two limits, for $\alpha_k \ll 1$,

$$\frac{\alpha_{k+1}}{\alpha_k} \sim \frac{\alpha_k}{2}. \quad (14)$$

$\alpha_k \gg 1$, we have

$$\alpha_{k+1} \sim \alpha_k - 1. \quad (15)$$

Since $\alpha_k \rightarrow 0$, we have $\theta_k \rightarrow \frac{\pi}{2}$. This ensures that $J_k \rightarrow 0$.

We evaluate the root mean square amplitude for this rf-field as $N \rightarrow \infty$

$$A_{eff} = w_0 \sqrt{\sum_{k=1}^N 2^{-k}} \sim \sqrt{2} w_0. \quad (16)$$

The ratio $\frac{2v_k}{\bar{w}_k}$ describes how well the oscillating component

$$\bar{w}_k \exp(j2v_k I_{z_k}) I_{x_k} \exp(-j2v_k I_{z_k}), \quad (17)$$

is averaged. This ratio

$$\frac{2v_k}{\bar{w}_k} = 2(\sqrt{\alpha_{k-1}^2 + 1} + 1) > 4. \quad (18)$$

$$\frac{v_k}{v_{k+1}} = \frac{\bar{w}_k}{\bar{w}_{k+1}} \frac{(\sqrt{\alpha_k^2 + 1} + 1)}{(\sqrt{\alpha_{k+1}^2 + 1} + 1)} > 2 \quad (19)$$

4 Non-Resonant Conditions

We now check whether all the oscillating terms captured by Hamiltonians H_k'' and H_k''' that were neglected result in an effective coupling. If this were to happen; in the modulation frame of the rf-field and chemical shifts, we will see a net coupling evolution. Therefore, we evaluate the evolution of the couplings in the modulation frame defined by the Hamiltonian $H_m = H_{cs} + H_{rf}$. The evolution of this frame takes the form

$$U(\omega, t) = \exp(-iv_1 I_{z_1(\omega)} t) \dots \exp(-iv_k I_{z_k(\omega)} t) \dots \exp(-iv_n I_{z_n(\omega)} t) \Theta_n(\omega, t),$$

Where

$$\dot{\Theta}_n(\omega) = -i\{f_n(\omega) I_{z(\omega)} + \tilde{H}(t)\} \Theta_n(\omega), \quad (20)$$

such that $|f_n(\omega)| \ll c_0$. Here $f_n(\omega)$ represents the chemical shift in the n^{th} frame. Where

$$\tilde{H}(t) = \sum_{k=1}^{N-1} V_{k+1}^\dagger H_k'' V_{k+1} \quad (21)$$

where

$$V_k(t) = \prod_{j=k}^N \exp(-iv_j I_{z_j} t). \quad (22)$$

In this notation,

$$U(\omega, t) = V_1(t) \Theta_n(\omega, t). \quad (23)$$

Where

$$\Theta_n(\omega, t) = I + \int_0^t \tilde{H}(\tau) d\tau + \int_0^t \int_0^\tau \tilde{H}(\tau) \tilde{H}(\sigma) d\tau d\sigma + \dots \quad (24)$$

Then in the frame of the Hamiltonian $H_m(t)$, the evolution takes the form

$$I - i2\pi J \int_0^t V_1' I_z S_z V_1 d\tau - 2\pi J \int_0^t \underbrace{[V_1' I_z S_z V_1, \int_0^\tau \tilde{H}(\sigma) d\sigma]}_{J(\tau)} d\tau + \dots \quad (25)$$

where, the first integral is averaged out in the subsequent frames as $\alpha_k \rightarrow 0$ and $v_k > 2v_{k+1}$ in Eq. (19) prevents generation of static components from the oscillating parts. We evaluate the second integral in the series above. If $J(\tau)$ has any static components this would reflect residual couplings in the system. We use the notation $H_k''(f)$ to denote the discrete set of frequencies present in oscillating Hamiltonian $H_k''(f)$. The discrete frequencies is the set

$$\{\exp(-i\omega I_\alpha) H_k'' \exp(i\omega I_\alpha)\}(f) = \{\omega \pm H_k''(f), \pm H_k''(f)\} \quad (26)$$

$$H_k''(f) = a_k v_k + \sum b_k v_{k+1}, a_k \in \{\pm 2\}, b_k \in \{0, \pm 1, \pm 2\}$$

Similarly, we have

$$V_1' I_z S_z V_1(f) = \sum_{k=1}^N c_k v_k,$$

where $c_k \in \{0, \pm 1\}$. We compute the overlap of the two set of frequencies, we find the smallest value of $|\Delta|$ satisfying

$$\sum_{j=1}^{k-1} c_j v_j + a_k v_k + \sum_{j=k+1}^N d_j v_j = \Delta \quad (27)$$

where $d_j \in \{0, \pm 1, \pm 2, \pm 3\}$. If $|\Delta| > 0$, we avoid a resonance condition.

4.1 Simulation and Experiments

Simulations were carried for a carbon-proton (IS) spin system, with a coupling constant $J = 140\text{ Hz}$ in Eq. (1). The Carbon chemical shift range was $c_0(2\pi)^{-1} = 22.5\text{ kHz}$, which corresponds to a 200 ppm Carbon chemical shift at 900 MHz proton frequency. At 6.25 kHz rf-power, the $\frac{\pi}{2}$ pulse corresponds to $40\text{ }\mu\text{s}$. We choose this as our A_{eff} in the MODE sequence, so that $\frac{c_0}{A_{eff}} = 3.6$. We choose $w_k = w_0$, and calculate w_0 that corresponds to $A_{eff} \sim 6.25\text{ kHz}$. For $N = 6$, this corresponds to $w_0 = 4.8\text{ kHz}$. Fig. 2 shows the amplitude and phase profile of the MODE sequence. Fig. 1 shows evolution of initial magnetization $S_x(0) = 1$ under the MODE sequence for various values of N for a period of $\sim 12J^-$. Fig. 1 also shows the decoupling efficiency,

$$\eta = \frac{1}{T} \int_0^T S_x(t) dt, \quad (28)$$

for various offsets.

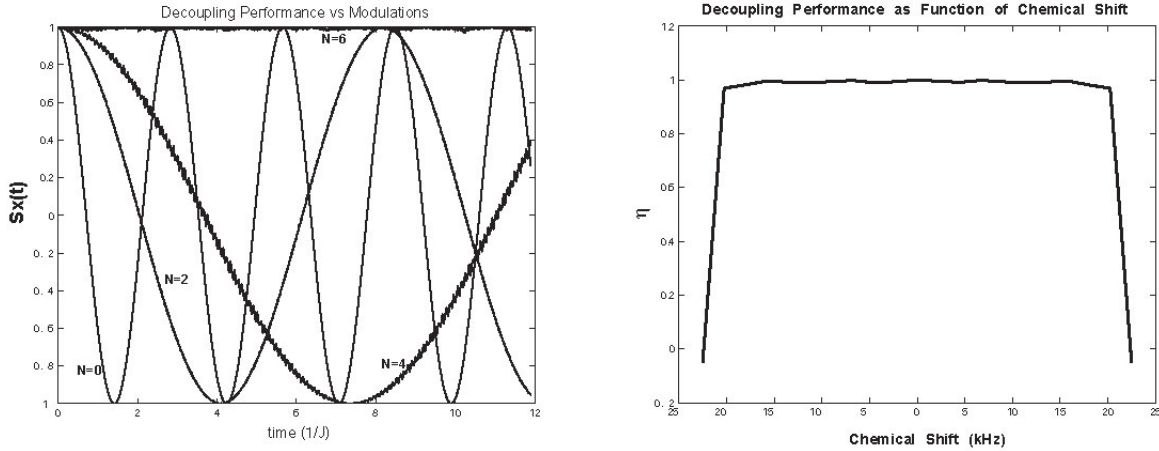


Figure 1: The left figure shows how the coherence $S_x(t)$ evolves as a function of time in units of J^- as N the number of modulations in the Rf-field are increased. The simulations correspond to $J = 140\text{ Hz}$, $A_{eff} \sim 6.25\text{ kHz}$ and $c_0 = 22.5\text{ kHz}$ corresponding to $\frac{c_0}{A_{eff}} = 3.6$ and the chemical shift value $\frac{\omega_0}{A_{eff}} = 1$. The right figure shows the decoupling efficiency $\eta = \frac{1}{T} \int_0^T S_x(t) dt$, as function of ω_0 . Here $T \sim \frac{12}{J} \sim 85\text{ ms}$.

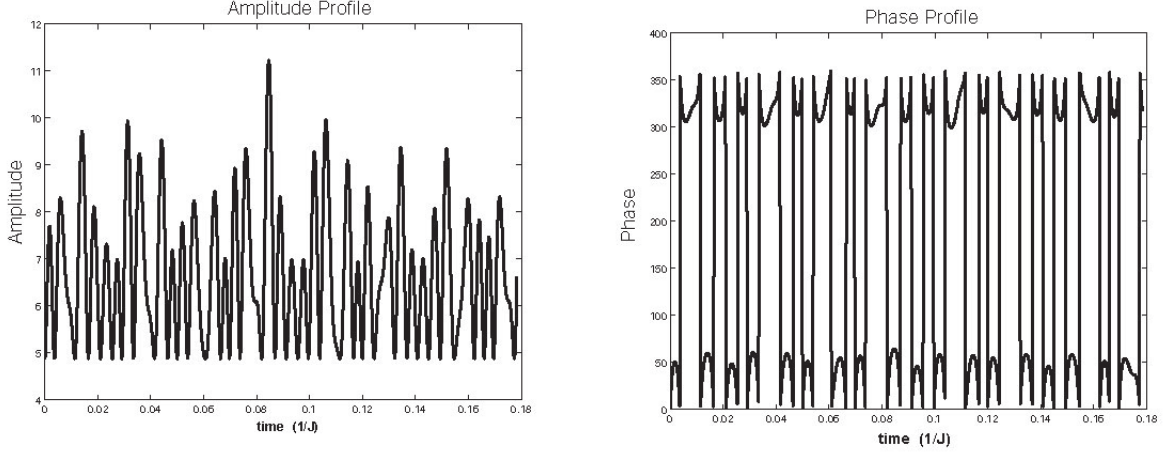


Figure 2: The top figure shows the Amplitude (in kHz) of the rf-field as a function of time in units of J^- , corresponding to $N = 6$ modulations, with $w_0 = 4.8$ kHz. This corresponds to $A_{eff} = 6.25$ kHz and the maximum amplitude $A_{max} = 12$ kHz. The bottom panel shows the phase (in degrees) as function of time.

The parameters of the MODE sequence for $N = 6$, $w_0 = 4.8$ kHz and $c_0 = 22.5$ kHz are $c_1 = 9.1$, $c_2 = 3.5$, $c_3 = 1.23$, $c_4 = .38$, $c_5 = .09$ and $c_6 = .01$ kHz. The ratio $\frac{c_0}{w_0} = 4.6$, $\frac{c_1}{w_1} = 3.7$, $\frac{c_2}{w_2} = 2.85$, $\frac{c_3}{w_3} = 2.02$, $\frac{c_4}{w_4} = 1.26$, $\frac{c_5}{w_5} = .61$ and $\frac{c_6}{w_6} = .17$. In the last frame the ratio of chemical shift to effective control is significantly reduced. The smallest frequency $|\Delta|$ in Eq. (27) is 197.3 Hz which avoids resonance.

Fig.(4) shows the experimental spectra obtained on a system of methyl Iodide with MODE sequence. The experimental parameters of the system are the same as in simulations. Comparison of conventional decoupling sequences with MODE shows it is much broadband for same root mean square rf-power. Fig.(5) shows the 2D HSQC spectra of the protein GB1, comparing GARP and MODE decoupling sequence on ^{13}C during direct detection.

The figure (3) shows the performance of the MODE decoupling sequence as function of rf-inhomogeneity, which is captured by the parameter $\epsilon = (1 + \delta)$, such that the actual amplitude of the rf field is ϵA where A is the nominal amplitude.

In the absence of inhomogeneity, for all $\omega \in [-c_0, c_0]$, $f_k(\omega) \leq f_k(c_0)$ and the ratio $\frac{c_k}{w_k}$ is

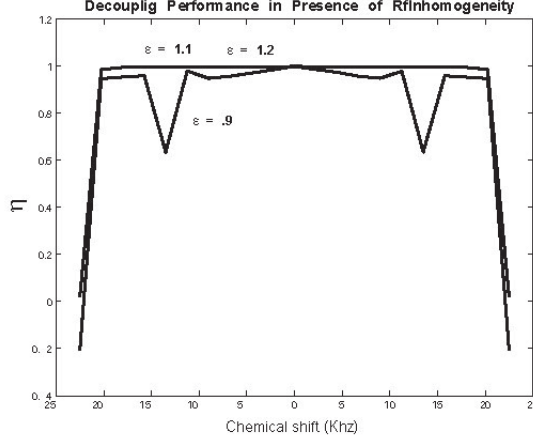


Figure 3: The above figure shows the decoupling efficiency η , as function of ω_0 . Here $T \sim \frac{12}{J} \sim 85$ ms for rf-inhomogeneity values corresponding to $\epsilon = .9$, $\epsilon = 1.1$ and $\epsilon = 1.2$ with $\delta = -.1$, $\delta = .1$ and $\delta = .2$ respectively. The mode sequence is designed with $N = 6$, $\frac{c_0}{w_0} = 3.6$ and $c_0 = 22.5$ kHz.

constantly decreasing. In the presence of rf-inhomogeneity, for our simulation with $\delta = .1$ and $\delta = .2$, it is observed that $\frac{f_k(c_0)}{\bar{w}_k}$ begins to increase. For $\delta = -.1$, we observe that $f_k(\omega) \not\leq f_k(c_0)$. The performance of the MODE sequence in presence of rf-inhomogeneity for $\delta > 0$ is comparable to the ideal case. For $\delta = -.1$ a small set of offsets are affected by rf-inhomogeneity. For these offsets, we find that the angle $\prod_k \cos(\theta_k)$ in 12 is the largest, indicating residual coupling in the system.

The following section discusses techniques to design in presence of rf-inhomogeneity.

5 Discussion and Conclusion

In the presence of rf-inhomogeneity, we can redefine our iterative procedure for computing the modulation frequencies ν_k . In presence of inhomogeneity, the spread of effective shifts after the first frame transformation is from $[(1-\delta)w_0, \sqrt{(1+\delta)^2 w_0^2 + c_0^2}]$, the left limit corresponds

to zero offset and smallest Rf-amplitude. The right limit corresponds to largest Rf-amplitude and chemical shift. We choose v_1 as center of this spread. Following this we obtain that

$$v_{k+1} = \frac{\sqrt{c_k^2 + \bar{w}_k^2(1+\delta)^2} + \bar{w}_k(1-\delta)}{2}; \quad c_{k+1} = \frac{\sqrt{c_k^2 + \bar{w}_k^2(1+\delta)^2} - \bar{w}_k(1-\delta)}{2}. \quad (29)$$

This gives

$$\alpha_{k+1} = \sqrt{\alpha_k^2 + (1+\delta)^2} - (1-\delta). \quad (30)$$

Note

$$\sqrt{\alpha_k^2 + (1+\delta)^2} - (1-\delta) \geq \alpha_k \quad (31)$$

with equality when

$$\alpha_k = \alpha_p = \frac{2\delta}{1-\delta}.$$

The α_k values decrease until they reach α_p . For $\delta = .1$, we have $\alpha_p \sim .22$, which is good enough as the ratio of chemical shift to Rf-strength is small. More generally, taking $w_{k+1} = \frac{w_k}{2g_k}$, we can move this fixed point close to zero.

In this paper, we introduced the multiple rotating field technique as a means to design broadband heteronuclear decoupling sequences in Solution NMR. It is important to point out that the MODE sequences for the case when $N = 1$, simply reduce to the well known TPPM decoupling pulse sequence [1]. Also see [2, 3, 4, 5, 6, 7]. The main contribution of this paper lies in realizing the importance of the ratio α_k and showing that by adding extra modulations in the rf-field and successively transforming into rotating frames, we can significantly reduce the ratio α_k and improve the decoupling performance. The technique is also expected to find use in designing decoupling pulse sequences in Solid State NMR and design of various excitation, inversion and mixing sequences, where spread of chemical shifts can simply be removed by transforming into a suitable K frame.

6 Acknowledgement

Authors would like to thank Prof. Steffen J. Glaser for helpful discussions on the subject and pointing out a complete set of references [56]. N. Khaneja will like to acknowledge NSF-0724057, ONR 38A-1077404 and AFOSR FA9550-05-1-0443 for supporting this work.

References

- [1] A.E. Benett, C.M. Rienstra, M. Auger, K.V. Lakshmi, R.G. Griffin, J. Chem. Phys. 103(1995)6951.
- [2] B. M. Fung, A. K. Khitrin, K. Ermolaev, J. Magn. Reson. 142(2000)97.
- [3] Z.H. Gan, R. R. Ernst, Solid State NMR 8(1997) 153.
- [4] M. Eden, M. H. Levitt, J. Chem. Phys. 111(1999) 1511.
- [5] Y. Yu, M. M. Fung, J. Magn. Reson. 130(1998) 317.
- [6] K. Takegoshi, J. Mizokami, T. Terao, Chem. Phys. Lett. 341(2001) 540.
- [7] A. Detken, E. Hardy, M. Ernst, B. Meier, Chem. Phys. Lett. 356(2002) 298-304.
- [8] M.H. Levitt, R. Freeman, T.A. Frenkiel, Broadband decoupling in high-resolution NMR spectroscopy, Adv. Magn. Reson. 11 (1983) 47-110.
- [9] A.J. Shaka, J. Keeler, Broadband spin decoupling in isotropic liquids, Prog. NMR Spectrosc. 19 (1987) 47-129.
- [10] W.A. Anderson, R. Freeman, Influence of a second radiofrequency field on high-resolution nuclear magnetic resonance spectra, J. Chem. Phys. 37 (1962) 85-103.
- [11] W.A. Anderson, F.A. Nelson, Removal of residual splitting in nuclear magnetic double resonance, J. Chem. Phys. 39, (1963) 183-189.

- [12] R.R. Ernst, Nuclear magnetic double resonance with an incoherent radio- frequency field, J. Chem. Phys. 45 (1966) 3845-3861.
- [13] R. Freeman, S.P. Kempsell, M.H. Levitt, Broadband decoupling and scaling of heteronuclear spin-spin interactions in high-resolution NMR", J. Magn. Reson. 35 (1979) 447-450.
- [14] M.H. Levitt, R. Freeman, T. Frenkiel, Broadband heteronuclear decoupling, J. Magn. Reson. 47 (1982) 328-330.
- [15] J.S. Waugh, Theory of broadband spin decoupling, J. Magn. Reson. 50 (1982) 30-49.
- [16] A.J. Shaka, J. Keeler, T. Frenkiel, and R. Freeman, An improved sequence for broadband decoupling: WALTZ-16, J. Magn. Reson. 52 (1983) 335-338.
- [17] A.J. Shaka, J. Keeler, R. Freeman, Evaluation of a new broadband decoupling sequence: WALTZ-16, J. Magn. Reson. 53, (1983) 313-340.
- [18] A.J. Shaka, P.B. Barker, R. Freeman, Computer-optimized decoupling scheme for wide-band applications and low-level operation, J. Magn. Reson. 64 (1985) 547-552.
- [19] T. Fujiwara, K. Nagayama, Composite inversion pulses with frequency switching and their application to broadband decoupling, J. Magn. Reson. 77 (1988) 53-63.
- [20] E.R.P. Zuiderweg, S.W. Fesik, Band-selective heteronuclear decoupling using shaped pulses as an aid in measuring long-range heteronuclear coupling constants, J. Magn. Reson. 93 (1991) 653-658.
- [21] U. Eggenberger, P. Schmidt, M. Sattler, S. J. Glaser, C. Griesinger, Frequency-Selective Decoupling with Recursively Expanded Soft Pulses in Multinuclear NMR, J. Magn. Reson. 100 (1992) 604-610.
- [22] M.A. McCoy, L. Mueller, Selective decoupling, J. Magn. Reson. A 101 (1993) 122-130.

- [23] T. Fujiwara, T. Anai, N. Kurihara, K. Nagayama, Frequency-switched composite pulses for decoupling carbon-13 spins over ultrabroad bandwidths, *J. Magn. Reson. A* 104 (1993) 103-105.
- [24] Z. Starcuk Jr., K. Bartusek, Z. Starcuk, Heteronuclear broadband spin-flip decoupling with adiabatic pulses, *J. Magn. Reson. A* 107 (1994) 24-31.
- [25] M.R. Bendall, Broadband and narrowband spin decoupling using adiabatic spin flips, *J. Magn. Reson. A* 112 (1995) 26-129.
- [26] T.E. Skinner, M.R. Bendall, Peak Power and Efficiency in Hyperbolic Secant Decoupling, *J. Magn. Reson. A* 123 (1995) 111-115.
- [27] E. Kupce, R. Freeman, Optimized adiabatic pulses for wideband spin inversion, *J. Magn. Reson. A* 118 (1996) 299-303.
- [28] R. Fu, G. Bodenhausen, Evaluation of adiabatic frequency-modulated schemes for broadband decoupling in isotropic liquids, *J. Magn. Reson. A* 119 (1996) 129-133.
- [29] H. Geen Theoretical design of amplitude-modulated pulses for spin decoupling in nuclear magnetic resonance, *J. Phys. B* 29 (1996) 1699-1710.
- [30] H. Geen, J.-M. Böhlen, Amplitude-modulated decoupling pulses in liquid state NMR, *J. Magn. Reson.* 125 (1997) 376-382.
- [31] P.A. Bottomley, C.J. Hardy, P.B. Roemer, O.M. Mueller, Proton-decoupled, Overhauser-enhanced, spatially localized carbon-13 spectroscopy in humans, *Magn. Reson. Med.* 12 (1989) 348-363.
- [32] D.M. Freeman, R. Hurd, Decoupling: theory and practice II. State of the art in vivo applications of decoupling, *NMR Biomed.* 10 (1997) 381-393.
- [33] P.B. Barker, X. Golay, D. Artemor, R. Ouwerkerk, M.A. Smith, A.J. Shaka, Broadband proton decoupling for in vivo brain spectroscopy in humans, *Magn. Reson. Med.* 45 (2001) 226-232.

- [34] R.A. de Graaf, Theoretical and experimental evaluation of broadband decoupling techniques for in vivo nuclear magnetic resonance spectroscopy, *Magn. Reson. Med.* 53 (2005) 1297-1306.
- [35] S. Li, J. Yang, J. Shen, Novel strategy for cerebral ^{13}C MRS using very low rf power for proton decoupling, *Magn. Reson. Med.* 57 (2007) 265-271.
- [36] A.P. Chen, J. Tropp, R. E. Hurd, M. Van Criekinge, L.G. Carvajal, D. Xu, J. Kurhanewicz, D.B. Vigneron, *In vivo* hyperpolarized ^{13}C MR spectroscopy imaging with ^1H decoupling, *J. Magn. Reson.* 197 (2009) 100-106.
- [37] M.H. Levitt, R. Freeman, T. Frenkiel, Supercycles for broadband heteronuclear decoupling, *J. Magn. Reson.* 50 (1982) 157-160.
- [38] M.H. Levitt, R.R. Ernst, Composite pulses constructed by a recursive expansion procedure, *J. Magn. Reson.* 55 (1983) 247-254.
- [39] R. Tycko, A. Pines, Fixed point theory of iterative excitation schemes in NMR, *J. Chem. Phys.* 83 (1985) 2775-2802.
- [40] H.M. Cho, R. Tycko, and A. Pines, Iterative maps for bistable excitation of two-level systems, *Phys. Rev. Lett.* 56 (1985) 1905-1908.
- [41] R. Tycko, Iterative methods in the design of pulse sequences for NMR excitation", *Adv. Magn. Reson.* 15 (Academic Press, New York, 1990).
- [42] J.J. Kotyk, J.R. Garbow, T. Gullion, Improvements in proton-detected NMR spectroscopy using spin-flip decoupling. An application to heteronuclear chemical shift correlation, *J. Magn. Reson.* 89 (1990) 647-653.
- [43] M.J. Lizak, T. Gullion, M.S. Conradi, Measurement of like-spin dipole couplings, *J. Magn. Reson.* 91 (1991) 254-260.

- [44] U. Haeberlen, J.S. Waugh, Coherent averaging effects in magnetic resonance, *Phys. Rev.* 175 (1968) 453-467.
- [45] U. Haeberlen, High Resolution NMR in solids: Selective Averaging, *Adv. Magn. Reson. Suppl.* 1 (1976).
- [46] R.R. Ernst, G. Bodenhausen, A. Wokaun, Principles of Nuclear Magnetic Resonance in One and Two Dimensions, Oxford, Clarendon Press (1987).
- [47] J. Cavanagh, W.J. Fairbrother, A.G. Palmer III, N.J. Skelton, Protein NMR Spectroscopy, New York, Academic Press (1996).
- [48] S.J. Glaser, J.J. Quant, Homonuclear and heteronuclear Hartmann-Hahn transfer in isotropic liquids, *Adv. in Magn. Opt. Reson.* 19, 59-252, San Diego, Academic Press (1996).
- [49] R.W. Dykstra, A method to suppress cycling sidebands in broadband decoupling, *J. Magn. Reson.* 82 (1989) 347-351.
- [50] E. Kupce, R. Freeman, G. Wider, K. Wüthrich, Suppression of cycling sidebands using bi-level adiabatic decoupling, *J. Magn. Reson. A* 122 (1996) 81-84.
- [51] T.E. Skinner, M.R. Bendall, A phase-cycling algorithm for reducing sidebands in adiabatic decoupling, *J. Magn. Reson.* 124 (1997) 474-478.
- [52] S. Zhang, D. Gorenstein, Adiabatic decoupling sidebands, *J. Magn. Reson.* 144 (2000) 316-321.
- [53] Z. Zhou, R. Kümmerle, X. Qiu, D. Redwine, R. Cong, A. Taha, D. Baugh, B. Winniford, A new decoupling method for accurate quantification of polyethylene copolymer composition and triad sequence distribution with ^{13}C NMR, *J. Magn. Reson.* 187 (2007) 225-233.

- [54] A.J. Shaka, P.B. Barker, R. Freeman, Three-spin effects in broadband decoupling, J. Magn. Reson. 71 (1987) 520-531.
- [55] D. Suter, V. Schenker, A. Pines, Theory of broadband heteronuclear decoupling in multispin systems, J. Magn. Reson. 73 (1987) 90-98.
- [56] J. Neves, B. Heitmann, N. Khaneja, S. J. Glaser, Heteronuclear decoupling by optimal tracking, J. Magn. Reson. 201 (2009) 7-17.

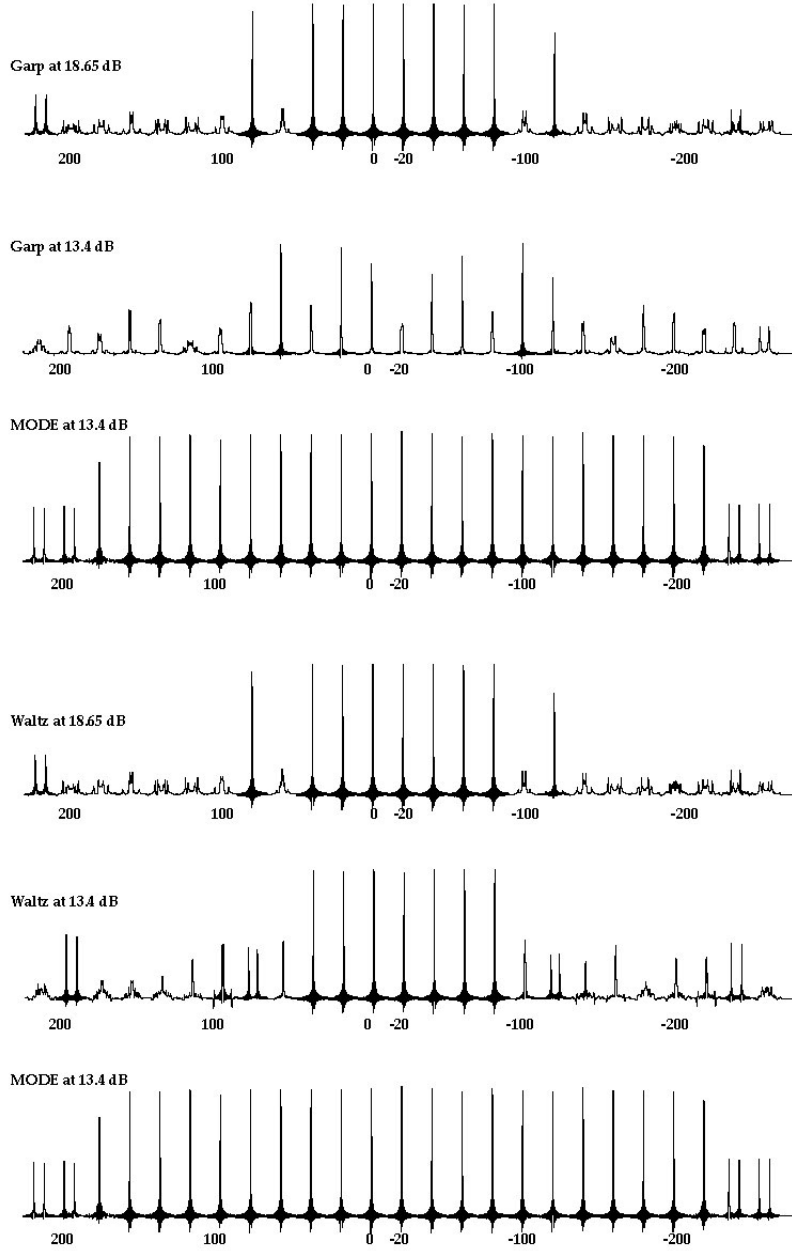


Figure 4: The above figures show the experimental proton spectra obtained at 500 mHz for a ^{13}C -iodomethane sample, dissolved in D-chloroform (D, 99.8%, Cambridge Isotope Laboratory, Inc.) The rf-field corresponds exactly to the simulation parameters with $N = 6$. The power level of 13.4 dB corresponds to a $40 \mu\text{s } \frac{\pi}{2}$ pulse. i.e, a 6.25 kHz Rf-field. The A_{eff} for the MODE decoupling sequence is at 6.25 kHz.

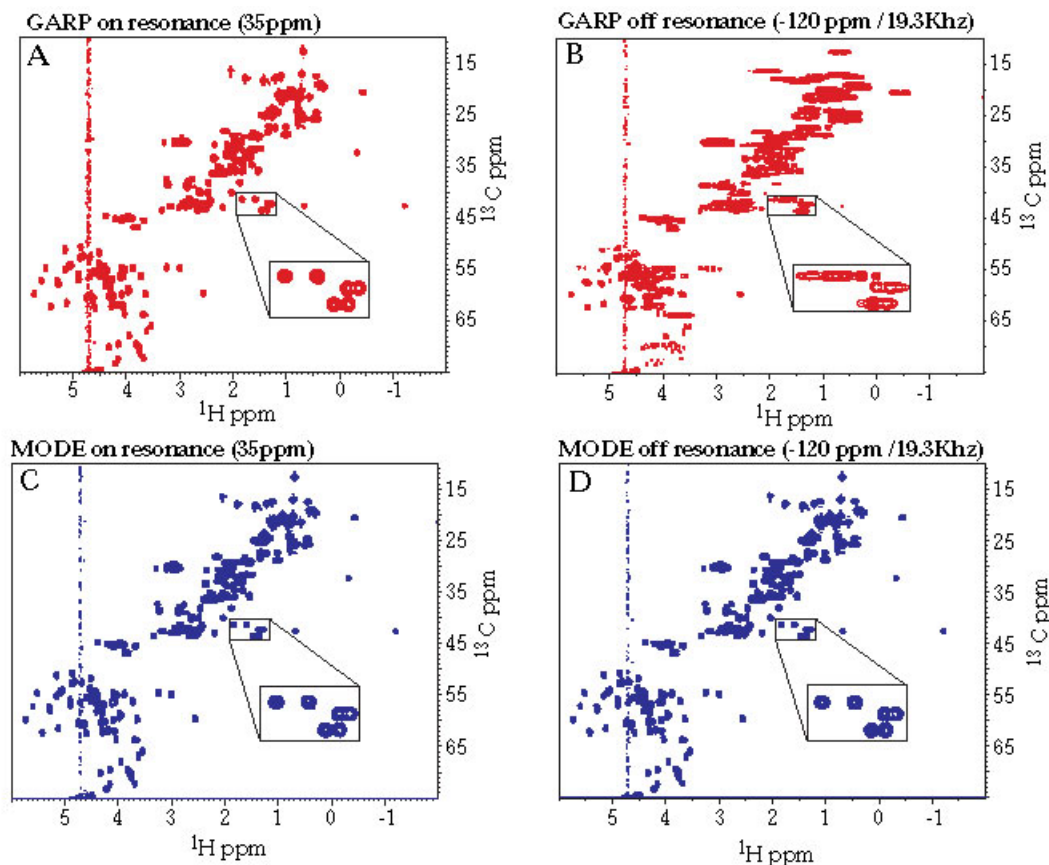


Figure 5: The above figures show the HSQC spectra on a sample of the protein GB1 obtained at 500 MHz. In the indirect dimension, the proton is decoupled by a refocusing π pulse. In the direct dimension, the carbon is decoupled by application of GARP and MODE decoupling sequences with mean rf-amplitude of ~ 3.68 kHz and 6.25 kHz respectively. The MODE sequence used is the same described earlier in the section. A plasmid pET30-a containing the gene coding for the HIS-tagged GB1 protein (59 amino acid immunoglobulin binding domain from streptococcal protein G) was transformed into *E. coli* BL21(DE3) cells for protein expression. A $^{15}\text{N}/^{13}\text{C}$ uniformly labeled sample was prepared by overexpression in M9 minimal media containing ^{13}C glucose and $^{15}\text{NH}_4\text{Cl}$. The protein was initially purified using a Nickel resin (Qiagen). The HIS tag was later removed with TEV protease and the resulting GB1 was further purified on a FPLC using a Sephadex column. The sample was concentrated to a final concentration of 1 mM in phosphate buffer (20 mM, pH = 6.5) with 150 mM NaCl and 100 M EDTA.